A simple model to predict train-induced vibration: theoretical formulation and experimental validation.

Author: F. Rossi
Università degli Studi di Perugia, Dipartimento di Ingegneria Industriale, Via G.Duranti 1/A-4, 06125 Perugia. Tel: +39 0755853846, fax +39 0755853697, e-mail frossi@unipg.it

1. Introduction

Environmental impact assessments require the prediction of vibration induced by moving loads like trains or trucks [1] [2]. Except for complicated simulation procedures which require long time calculation and a huge amount of input data, no suitable method is however available to predict vibration values induced by train passage [3]. Thus, vibrations values are very often predicted without a mathematical method but simply describing possible macroscopic effect induced by vibration [4]. In this paper a useful simple method for train-induced vibration prediction is proposed. The method has been introduced for high speed trains. The model input data are train velocity, train mass, rail geometry, soil characteristics and prediction point-rail distance. The model output data is maximum soil particles r.m.s. velocities (longitudinal and transversal) and vibration level. Data are found adopting conservative assumptions; thus the predicted values constitute an upper limit to real measurable vibration values. The model has been calibrated by means of measurement results led along an Italian railway. Furthermore the model results have been compared to a big amount of vibration data retrieved from measurement campaigns led along high speed European rail lines. Comparison shows that, if soil properties are known or can be properly estimated, error associated to predicted level is lower than 2.5dB. Worst case most conservative condition has been identified in order to use the method when soil properties are not known.

2. Theoretical formulation

In order to estimate maximum soil particles r.m.s. velocities at a prediction point both vibration source and propagation phenomenon must be modeled.

2.1 Vibration source model

Energy transfer from vibration source (train and embankment) to soil is governed by complex mechanism the behavior of which is difficultly identifiable [5] [6]. Thus a simplifying hypothesis is introduced: a constant portion of the energy transferred by the traveling train to the ballast-embankment system is then retransferred to the surrounding soil. Such a hypothesis is verified if ballast-embankment system and junction elements are uniform allover the railway; thus the following statement may be written:

$$W = K \cdot W_T \qquad (1)$$

The constant K must be set by calibrating the model.
Power transferred by train to ballast-embankment system W_T depends on train velocity, train mass, train length and rail geometry. In order to determine W_T, train specific mass is introduced, defined as follows:

$$m = \frac{M}{T} \tag{2}$$

Energy transferred by train per unit of length is given by:

$$e = m \cdot g \cdot s \tag{3}$$

where s is the maximum vertical rail displacement admitted for a train passage [7] [8] [9]. Power is found assuming that energy is transferred to the ballast-embankment system by means of the sleepers; furthermore energy expressed by eq. (3) is release during the time the train takes to go from a sleeper to the next one. Thus the power associated to eq. (3) is given by:

$$\omega_T = m \cdot g \cdot s \cdot \frac{v_T}{i} \tag{4}$$

Power transferred to ballast-embankment system by a dx portion of train is:

$$d\omega_T = m \cdot g \cdot s \cdot \frac{v_T}{i} \cdot dx \tag{5}$$

According to eq. (1), power retransferred from the ballast-embankment system to the soil by a dx portion of train is given by:

$$d\omega = m \cdot g \cdot s \cdot \frac{v_T}{i} \cdot K \cdot dx \tag{6}$$

2.2 Propagation model

Maximum particles r.m.s. velocities are attained when train and prediction point are reciprocally located as shown in Fig.1. Embankment is considered to be a continuous semispherical emitting line the power density of which is given by eq.(5) [10] [11] [12] [13]. Vibration emission distribution is supposed semispherical because of the very great difference between air mechanical impedance and soil's one [14], thus energy directed toward air is mostly reflected and contributes to soil vibration (see fig.1); this fact is kept into account by doubling power transferred to soil [15]. Reflections caused by different impendence layers under soil surface are not kept into account; in fact, energy reflected by such layers is proportional to the layer interface reflection coefficient which assumes its maximum value when layers impedances assume respectively the maximum and the minimum admitted values.

$$\begin{aligned} R_{\max} &= \frac{z_{\max} - z_{\min}}{z_{\max} + z_{\min}}; \\ z_{\max} &= \sqrt{E_{\max} \cdot \rho_{\max}}; \\ z_{\min} &= \sqrt{E_{\min} \cdot \rho_{\min}} \end{aligned} \tag{7}$$

z_{min} and z_{min} are calculated with the minimum and the maximum admitted values for Young module and soil density: $E_{min}=30\cdot10^6$ Pa, $\rho_{min}=1.2\cdot10^3$ Kg/m^3; $E_{max}=100\cdot10^6$ Pa, $\rho_{max}=2.3\cdot10^3$ Kg/m^3 [16]. The maximum energy reflected by impedance discontinuity is therefore calculable by the following equation:

$$E_R = R^2 \cdot E_i \tag{8}$$

According to eq. (7), $R^2 = 0.18$. Maximum possible reflected energy is lower than 20% of the incident energy [17]. As it will be later discussed, such a percentage may be neglected when vibration level are introduced.

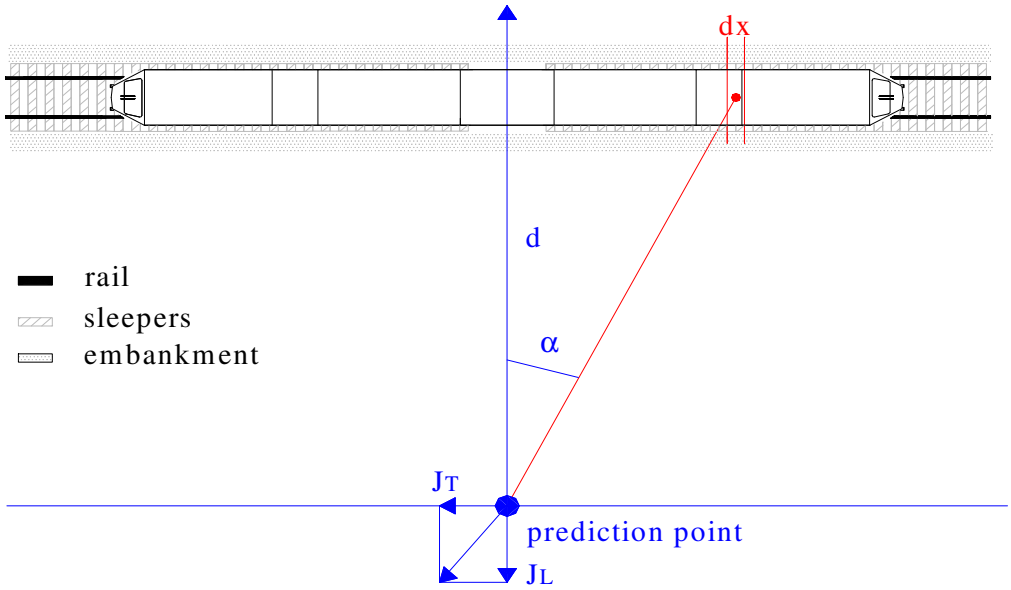

Fig.1: Model reference scheme

According to the previous hypothesis, power per unit of area which passes through a generic surface point P (see fig.1) is distributed between a longitudinal and a transversal component [18]. Each component can be found by considering the contribute of each train portion:

$$dJ_L = 2 \cdot \int_0^{\frac{T}{2}} \frac{2 \cdot d\omega \cdot \cos\alpha}{4\pi \cdot r^2}; \qquad dJ_T = 2 \cdot \int_0^{\frac{T}{2}} \frac{2 \cdot d\omega \cdot \sin\alpha}{4\pi \cdot r^2} \tag{9}$$

According to eq.(9), longitudinal and transversal powers per unit of area become:

$$dJ_L = \int_0^{\frac{T}{2}} \frac{m \cdot g \cdot s \cdot v_T \cdot K \cdot d}{\pi \cdot i \cdot \left(x^2 + d^2\right)^{3/2}} \cdot dx; \qquad dJ_T = \int_0^{\frac{T}{2}} \frac{m \cdot g \cdot s \cdot v_T \cdot K \cdot x}{\pi \cdot i \cdot \left(x^2 + d^2\right)^{3/2}} \cdot dx \tag{10}$$

Solving eq. (10):

$$J_L = \frac{m \cdot g \cdot s \cdot v_T \cdot K}{\pi \cdot i}\left(\frac{T}{d \cdot \sqrt{T^2 + 4d^2}}\right) \qquad J_T = \frac{m \cdot g \cdot s \cdot v_T \cdot K}{\pi \cdot i}\left(\frac{1}{d} - \frac{2}{\sqrt{T^2 + 4d^2}}\right) \tag{11}$$

Maximum particles r.m.s. velocity can be found for longitudinal and transversal waves by means of the following relations [19]:

$$u_L = \sqrt{\frac{J_L}{z_L}} \tag{12}$$

and:

$$u_T = \sqrt{\frac{J_T}{z_T}} \tag{13}$$

where:

$$\begin{aligned} z_L &= \sqrt{\rho \cdot D}; \quad \text{with} \quad D = \frac{E(1-\upsilon)}{(1+\upsilon)\cdot(1-2\upsilon)}; \\ z_T &= \sqrt{\rho \cdot G}; \quad \text{with} \quad G = \frac{E}{2(1+\upsilon)} \end{aligned} \tag{14}$$

Absolute value of particles r.m.s. velocity is attained by composing transversal and longitudinal velocities:

$$u = \sqrt{u_T^2 + u_L^2} \tag{15}$$

Absolute vibration level is then given by the following relation:

$$L = 20 \cdot \log\left(\frac{u}{u_{ref}}\right); \quad u_{ref} = 10^{-8} m/s \tag{16}$$

According to eq. (16), the maximum contribute caused by wave reflections on different impedance layers is estimable by the following relation:

$$L_{D+R} = 10 \cdot \log\left(\frac{E_i + R^2 E_i}{E_{ref}}\right) = L + 10 \cdot \log(1+R^2) = L + 0.7\text{dB} \tag{17}$$

It is assumed to neglect such a contribute for the following reasons:

1. 0.7 dB is a small value if compared to the absolute measured values;
2. 0.7 dB has been maximized in terms of possible soil types; furthermore it is also the maximum theoretical value which occurs only when all incident energy reaches the prediction point. This fact never happens.

3. Model calibration

The proposed model has been calibrated by means of measurements campaign. Calibration is needed in order to determine the value of constant *K* (see eq. (1)).

3.1 Measurement Campaign

Measurement points have been placed along a straight part of an high speed rail line sited close to Terontola Station in Italy (Rome-Florence stage); no bridge and no bend are located near the measurement points (see Fig.2). Vibrations have been measured at 5, 10, 20, 40 meters from the rail center line. Both transversal and longitudinal waves have been measured by means of geophones (models GS-30CT for longitudinal waves, GS-32CT for transversal waves) [20]. Geophones signals have been acquired and processed by means of OROS acquisition board connected to a custom DASY-LAB based code for vibration signal processing [21]. Signal processing allowed to calculate transversal and longitudinal particles r.m.s. velocities from the train-induced instantaneous velocities time history. Particles r.m.s. velocities values have been calculated by the code according to the following relation:

$$u_L = \frac{1}{N}\sum_{j=0}^{N} u_{L,j}; \quad with \quad u_{L,j} = \sqrt{\int_j^{j+1} v_{L,j}^2(t)\cdot dt}$$
$$u_T = \frac{1}{N}\sum_{j=0}^{N} u_{T,j}; \quad with \quad u_{T,j} = \sqrt{\int_j^{j+1} v_{T,j}^2(t)\cdot dt} \qquad (18)$$

The data processing system furnishes also a vibration level calculated on 1 second time interval. For the *j*-th 1 second time interval, vibration level is defined as follows:

$$L_j = 20\cdot\log\left(\frac{\sqrt{u_{L,j}^2 + u_{T,j}^2}}{u_{ref}}\right); \quad u_{ref} = 10^{-8}\, m/s \qquad (19)$$

The time N is the total measurement integration time which is different for each train passage. Within such an interval each 1 second vibration level L_j is higher than 10dB:

$$L_j > 10dB \qquad (20)$$

Condition (19) means that outside the N time interval train passage produces vibrations levels lower than 10dB.Vibration have been measured during ETR500 passage. ETR500 is an Italian high speed train the characteristics of which are: M=620·10^{3}Kg, T=328m. In Fig.3, Vibration level time history during ETR500 passage (speed 150Km/h, rail-point distance=10m) is shown; in that case N=20s. The soil which surrounds the measurement site is composed by compressed high density sands the characteristics of which are E=9·10^6 Pa and ν=0.2 [16] [22]. In Tab.1, measured r.m.s. velocities are shown for different train speed and at different measurement points.

Fig.2: Measurement site

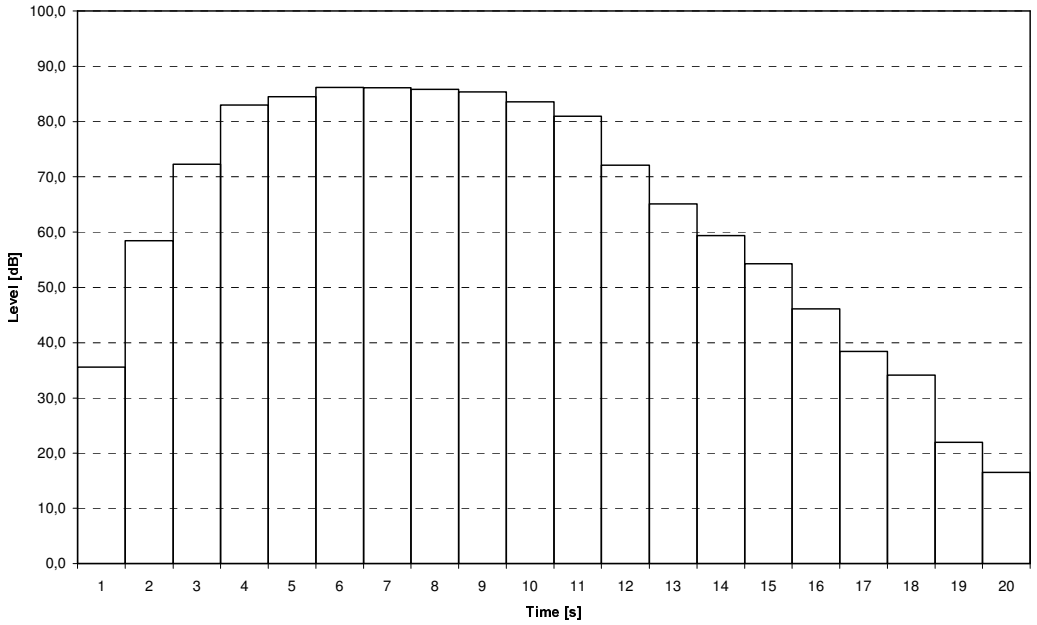

Fig.3: Vibration level time history during ETR500 passage (speed 150Km/h, rail-point distance=10m)

Tab.1: Measurement results: particles r.m.s. velocities values and vibration levels during ETR500 passage

Rail–point distance [m]	**Train speed [km/h]**								
	100			150			200		
	u_L 10^{-5} *[m/s]*	u_T 10^{-5} *[m/s]*	*L [dB]*	u_L 10^{-5} *[m/s]*	u_T 10^{-5} *[m/s]*	*L [dB]*	u_L 10^{-5} *[m/s]*	u_T 10^{-5} *[m/s]*	*L [dB]*
5	8.2	9.9	82.1	9.9	11.6	83.7	11.7	14.4	85.4
10	5.5	7.2	79.2	7.1	8.8	81.1	8.0	9.7	82.0
20	4.2	4.9	76.2	4.7	5.7	77.4	5.7	6.5	78.7
40	2.7	2.9	72.0	3.5	3.9	74.4	4.1	4.5	75.7

3.2 Calibration

The model has been calibrated by determining the value of K (see eq.(1)) which equalizes equations (12), (13) to the corresponding measured values. Calibration is carried out setting maximum rail vertical displacement $s=1\cdot10^{-2}$m which is the maximum admitted value [7]. For each different train speed, rail-point distance and wave component, the "equalizing" K assumes a different value. Each K is, however, very close to its average value $\underline{K}$ (see Tab.2). Thus the model may be calibrated setting:

$$K = \underline{K} = 5\cdot10^{-6} \qquad (20)$$

According to Tab.2, absolute maximum difference with respect to average is $|K-\underline{K}|_{max}=7.7\cdot10^{-7}$, and K standard deviation is $\sigma_K=3.3\cdot10^{-7}$. Calibrating the model according to (20), maximum error, in terms of predicted vibration level, is lower than 0.75dB.

Tab.2: Values of K which equalizes model result to measurement ones

Rail–point distance [m]	**Train velocity [km/h]**					
	100		***150***		***150***	
	Longitudinal	Transversal	Longitudinal	Transversal	Longitudinal	Transversal
5	$5.2\ 10^{-6}$	$4.8\ 10^{-6}$	$5.1\ 10^{-6}$	$4.4\ 10^{-6}$	$5.3\ 10^{-6}$	$5.1\ 10^{-6}$
10	$4.7\ 10^{-6}$	$5.3\ 10^{-6}$	$5.2\ 10^{-6}$	$5.2\ 10^{-6}$	$5.0\ 10^{-6}$	$4.8\ 10^{-6}$
20	$5.5\ 10^{-6}$	$5.2\ 10^{-6}$	$4.6\ 10^{-6}$	$4.7\ 10^{-6}$	$5.1\ 10^{-6}$	$4.6\ 10^{-6}$
40	$4.7\ 10^{-6}$	$4.2\ 10^{-6}$	$5.2\ 10^{-6}$	$5.1\ 10^{-6}$	$5.4\ 10^{-6}$	$5.0\ 10^{-6}$
Average $\underline{K} = 4.975\ 10^{-6} \approx 4.5\ 10^{-6}$ $\sigma_k = 3.3\ 10^{-7}$ $\lvert K-\underline{K}\rvert_{max} = 7.7\ 10^{-7}$						

According to the previous observation, K is supposed invariant for any high speed rail lines; it may be admitted because track ballast and embankment are characterized by the same construction criteria for any modern high speed railways [23].

4. Model validation

4.1 Method

Model predicted levels have been compared to the result of a measurement campaign led along the most important European high speed train railways [24]. The characteristics of trains the vibrations of which have been measured are shown in Tab.3. Measurement data are reported in terms of vibration levels which are available for different conditions (measurement point-rail distance, train speed, type of train).

Tab.3: High speed trains characteristics

Model	***Description***	***Moving Mass [Kg]***	***Length [m]***
Pendolino	Top speed: 250 Km/h Total power: 6.24 MW Configuration: 9 trailers Home: Italy	$450 \cdot 10^3$	236
EuroStar	Top speed: 300 Km/h Total power: 12.2 MW Configuration: 1 power car + 18 trailers + 1 power car Home: France	$770 \cdot 10^3$	394
TGV (Atlantique)	Top speed: 300 Km/h Total power: 8.8 MW Configuration: 1 power car + 10 trailers + 1 power car Home: France	$500 \cdot 10^3$	238
TGV (North)	Top speed: 300 Km/h Total power: 8.8 MW Configuration: 1 power car + 10 trailers + 1 power car Home: France	$400 \cdot 10^3$	200
X2000	Top speed: 210 Km/h Configuration: 1 power unit, 3 passenger cars, 1 bistro car and 1 cab car Home: Sweden	$375 \cdot 10^3$	165

Comparison between model and measurement results has been carried out assuming that high speed train railways are built on a compressed high density soil the properties of

which may be supposed to be $E=90\cdot10^6$Pa and $\rho=1.8\cdot10^3$Kg/m^3; this assumption has been taken into account because no soil properties of the measurement sites are given [24]. Furthermore it may be simply shown that model results depends very weakly on Poisson ratio (maximum error in terms of vibration level is lower than 0.1dB if $\nu=0.3$ rather than $\nu=0.18$); thus, for each case, it may be errorless assumed $\nu=0.2$ [16]. Although the previous assumptions are sustainable, the worst prediction case is also investigated in order to establish the maximum error on predicted vibration levels when no hypothesis about soil can be assumed. Worst prediction case occurs when the difference between a predicted level and a measured one is the maximum admitted. It may be observed (see eq. (12), (13) and (15)) that vibration level depends on Young module and on soil density like a descending monotonic function; thus maximum difference between a predicted level and a measured one occurs when Young module and soil density assumes contemporarily the minimum admitted values or, alternatively, the maximum ones. Furthermore, adopting Young Module and soil density minimum values, maximum predictable levels are attained.

4.2 Measurement results and model comparison

In Tab.4, vibration levels produced by some of the most important European high speed trains are reported. Because of the different characteristics among the 5 types of trains, vibration levels measurements have been carried out not for the same train speeds but for each single train generally practiced speed [25] [26]. Also the measurement distances are difference for each case. In Tab.5, vibration levels predicted by the proposed model are shown. Prediction has been made inputting the model with the train characteristics of Tab.3 under geometrical and train speed conditions which are the same as the measurement ones. If compressed high density soil is considered (assumption $E=90\cdot10^6$Pa, $\rho=1.8\cdot10^3$Kg/m^3) for each prediction case, the differences between predicted and measured levels are very small (see Tab.5): the average difference is $\underline{\Delta}=1.0$dB while the maximum difference between a predicted level and the corresponding measured one is $\Delta_{max}=2.5$dB. Probably, if soil properties were known, errors could be even lower.

Tab.4: Vibration level measured along some European railways during the passage of high speed trains [24].

Pendolino				
Measure point-railway distance [m]	Speed [km/h]			
	240	**200**	**160**	
10	83.6	82.1	80.1	dB
25	78.7	77.2	75.2	
45	75.3	73.8	71.8	
Eurostar				
Measure point-railway distance [m]	Speed [km/h]			
	260	**200**	**160**	
18	81.8	79.6	77.6	dB
25	80.0	77.8	75.8	
55	75.2	73.0	71.0	
TGV Atlantique				
Measure point-railway distance [m]	Speed [km/h]			
	260	**200**	**160**	
25	79.2	77.0	75.0	dB
30	78.2	76.0	74.0	

100	70.5	68.3	66.3	
TGV North				
Measure point-railway distance [m]	Speed [km/h]			
	260	**200**	**160**	
18	81.6	79.4	77.4	dB
25	78.5	76.3	74.3	
55	74.2	72.0	70.0	
X2000				
Measure point-railway distance [m]	Speed [km/h]			
	190	**160**	**120**	
20	79.0	77.5	75.0	dB
40	75.9	74.4	71.9	
60	72.4	70.9	68.4	

Tab.5: Vibration levels predicted by the proposed model for some European high speed trains. Difference Δ between predicted and measured values.

Pendolino						
Prediction point-railway distance [m]	Speed [km/h]					
	240		200		160	
	L [dB]	Δ [dB]	L [dB]	Δ [dB]	L [dB]	Δ [dB]
10	82.9	- 0.8	82.1	+0.0	81.1	+1.0
25	78.5	- 0.3	77.7	+0.5	76.7	+1.5
45	75.4	+0.0	74.6	+0.8	73.6	+1.8
Eurostar						
Prediction point-railway distance [m]	Speed [km/h]					
	260		200		160	
	L [dB]	Δ [dB]	L [dB]	Δ [dB]	L [dB]	Δ [dB]
18	80.8	- 1.1	79.6	+0.0	78.7	+1.0
25	79.2	- 0.8	78.1	+0.3	77.1	+1.3
55	75.3	+0.1	74.2	+1.2	73.2	+2.2
TGV Atlantique						
Prediction point-railway distance [m]	Speed [km/h]					
	260		200		160	
	L [dB]	Δ [dB]	L [dB]	Δ [dB]	L [dB]	Δ [dB]
25	79.3	+0.0	78.1	+1.2	77.2	+2.1
30	78.5	+0.3	77.4	+1.4	76.4	+2.4
100	71.0	+0.4	69.8	+1.6	68.9	+2.5
TGV North						
Prediction point-railway distance [m]	Speed [km/h]					
	260		200		160	
	L [dB]	Δ [dB]	L [dB]	Δ [dB]	L [dB]	Δ [dB]
18	80.6	- 1.1	79.4	+0.1	78.5	+1.1
25	78.9	+0.4	77.8	+1.5	76.8	+2.5
55	74.4	+0.2	73.3	+1.3	72.3	+2.3
X2000						
Prediction point-railway distance [m]	Speed [km/h]					
	190		160		120	
	L [dB]	Δ [dB]	L [dB]	Δ [dB]	L [dB]	Δ [dB]
20	79.1	+0.1	78.4	+0.8	77.1	+2.1
40	75.2	- 0.7	75.5	+0.1	73.2	+1.3
60	72.6	+0.2	71.8	+0.9	70.6	+2.2

It may be also shown that just 6 of the whole 45 predicted levels are lower than the corresponding measured level. It is due to the conservative approach on hypothesis adoption. In Tab.6, worst case predicted levels are shown. It may be simply proved that worst case occurs when both Young Module and soil density assumes their minimum admitted values (E_{min}=30·10^{6}Pa, ρ_{min}=1.2·10^{3}Kg/m^3) [16]. Worst case average difference between predicted and measured levels is $\underline{\Delta}_{wr}$=4.1dB while the maximum difference between a predicted level and the corresponding measured one is $\Delta_{max,wr}$=5.8dB. Each predicted level of Tab.6 is higher than the corresponding measured one; thus, because of the dependence of vibration level on Young Module and soil density (see eq (12),(13), (16)), worst case constitutes also the most conservative case.

Tab.6: Worst case condition: vibration levels predicted by the proposed model and difference Δ between predicted and measured values.

Pendolino						
Prediction point-railway distance [m]	Speed [km/h]					
	240		200		160	
	L [dB]	Δ_{wr} [dB]	L [dB]	Δ_{wr} [dB]	L [dB]	Δ_{wr} [dB]
10	86.1	+2.5	85.4	+3.3	84.4	+4.3
25	81.8	+3.0	81.0	+3.8	80.0	+4.8
45	78.6	+3.3	77.8	+4.1	76.9	+5.0
Eurostar						
Prediction point-railway distance [m]	Speed [km/h]					
	260		200		160	
	L [dB]	Δ_{wr} [dB]	L [dB]	Δ_{wr} [dB]	L [dB]	Δ_{wr} [dB]
18	84.0	+ 2.2	82.9	+3.3	81.9	+4.3
25	82.5	+2.4	81.4	+3.6	80.4	+4.6
55	78.6	+3.3	77.4	+4.5	76.5	+5.4
TGV Atlantique						
Prediction point-railway distance [m]	Speed [km/h]					
	260		200		160	
	L [dB]	Δ_{wr} [dB]	L [dB]	Δ_{wr} [dB]	L [dB]	Δ_{wr} [dB]
25	82.5	+3.3	81.4	+4.4	80.4	+5.4
30	81.6	+3.4	80.5	+4.5	79.5	+5.5
100	74.2	+3.7	73.1	+4.8	72.1	+5.8
TGV North						
Prediction point-railway distance [m]	Speed [km/h]					
	260		200		160	
	L [dB]	Δ_{wr} [dB]	L [dB]	Δ_{wr} [dB]	L [dB]	Δ_{wr} [dB]
18	83.9	+2.2	82.7	+3.3	81.7	+4.3
25	82.2	+3.6	81.1	+4.8	80.1	+5.8
55	77.7	+3.5	76.6	+4.6	70.0	+5.6
X2000						
Prediction point-railway distance [m]	Speed [km/h]					
	190		160		120	
	L [dB]	Δ_{wr} [dB]	L [dB]	Δ_{wr} [dB]	L [dB]	Δ_{wr} [dB]
20	82.4	+3.4	81.6	+4.1	80.4	+5.4
40	78.5	+2.6	77.6	+3.2	76.5	+4.6
60	75.9	+3.4	75.1	+4.2	73.9	+5.4

5. Conclusions

The proposed model for train-induced soil vibration prediction furnishes r.m.s. velocities (longitudinal and transversal) and global vibration level. The model has been calibrated by means of a measurement campaign conducted along an Italian high speed railway during ETR 500 passage. The model was then validated comparing it to a great amount of vibration data retrieved from the reports of some experimental investigations led along the most important European high speed railways.

Comparison between predicted and measured levels were made without the knowledge of the soil properties; so the hypothesis of compressed high density soil ($E=90\cdot10^6$Pa, $\rho=1.8\cdot10^3$Kg/m^3) was adopted. The very small difference ($\underline{\Delta}=1.0$dB, $\Delta_{max}=2.5$dB) between predicted and measured levels suggests the following considerations:

1. the calibration value of constant *K* may be considered unique for any high speed railways.
2. The assumption of compressed high density soil for high speed railways is sustainable when no specific data on soil property is known.
3. The knowledge of soil properties specific data could lead to more accurate predicted levels.

Worst case prediction levels were also compared to the measured ones. The difference ($\underline{\Delta}_{wr}=4.1$dB, $\Delta_{max,wr}=5.8$dB) between predicted and measured levels suggests the following considerations:

4. when no hypothesis may be assumed about soil properties, the proposed model may be used under worst case condition which occurs when both Young Module and soil density assumes their minimum admitted values ($E=30\cdot10^6$Pa, $\rho=1.2\cdot10^3$Kg/m^3).
5. Furthermore, if minimum admitted values are assigned to Young Module and soil density, the model furnishes the higher predictable vibration levels: this fact constitutes the most conservative condition which can be used as preliminary Prediction Survey Method.

The proposed model may be conveniently employed to predict train-induced vibration committing a very small error when soil properties are known. Anyway a worst case condition, which is also the most conservative, may be assumed in absence of soil properties data. The method may be particularly important on vibration impact assessment.

6. Table of symbols

Symbol	Units	Description
α	rad	construction angle (see Fig.1)
D	Pa	soil longitudinal rigidity
d	m	minimum distance between rail and prediction point
$\underline{\Delta}$	dB	average difference between predicted and measured levels
Δ_{max}	dB	maximum difference between predicted and measured levels

$\Delta_{max,wr}$	dB	worst case: maximum difference between predicted and measured levels
Δ_{wr}	dB	worst case: average difference between predicted and measured levels
E	Pa	soil Young module
E_i	J	incident energy
E_{max}	Pa	maximum soil Young module
E_{min}	Pa	minimum soil Young module
E_R	J	reflected energy
E_{ref}	J	reference energy
e	$J \cdot m^{-1}$	energy transferred by train to ballast-embankment system per unit of length
G	Pa	Soil torsional elasticity module
g	$m \cdot s^{-2}$	gravity acceleration
i	m	distance between two consecutive sleepers
J_L	$W \cdot m^{-2}$	power longitudinal component transferred by train to surrounding soil
J_T	$W \cdot m^{-2}$	power transversal component transferred by train to surrounding soil
K	adimensional	model calibrating constant
$\underline{K}$	adimensional	model calibrating average constant
$\lvert K-\underline{K}\rvert_{max}$	adimensional	absolute maximum difference between K and $\underline{K}$
L	dB	absolute vibration level
L_{D+R}	dB	vibration level due to direct and reflected waves
L_j	dB	vibration level referred to a 1 second time interval
M	Kg	train total mass
m	$Kg \cdot m^{-1}$	train specific mass
R_{max}	adimensional	maximum reflection coefficient
r	m	distance between a soil surface point and a source point
ρ	$Kg \cdot m^{-3}$	soil density
ρ_{max}	$Kg \cdot m^{-3}$	maximum soil density
ρ_{min}	$Kg \cdot m^{-3}$	minimum soil density
s	m	maximum vertical rail displacement
σ_K	adimensional	K standard deviation
T	m	train length
u	$m \cdot s^{-1}$	maximum particles r.m.s. velocity
u_L	$m \cdot s^{-1}$	particles r.m.s. longitudinal velocity component
$u_{L,j}$	$m \cdot s^{-1}$	particles r.m.s. longitudinal velocity component referred to

		a 1 second time interval
u_T	m ·s^{-1}	particles r.m.s. transversal velocity component
$u_{T,j}$	m ·s^{-1}	particles r.m.s. transversal velocity component referred to a 1 second time interval
u_{ref}	m ·s^{-1}	reference particles velocity
υ	adimensional	soil Poisson's ratio
$v_{L,j}$	m ·s^{-1}	particles instantaneous longitudinal velocity
v_T	m ·s^{-1}	train speed
$v_{T,j}$	m ·s^{-1}	particles instantaneous transversal velocity
W	W	power transferred by train to surrounding soil
W_T	W	power transferred by train to ballast-embankment
ω_T	W·m^{-1}	power transferred by train to ballast-embankment per unit of length
ω	W	power transferred by train to surrounding soil
x	m	portion of train
z_L	Kg ·m^{-2} ·s^{-1}	longitudinal mechanical impedance
z_{max}	Kg ·m^{-2} ·s^{-1}	maximum soil layer impedance
z_{min}	Kg ·m^{-2} ·s^{-1}	minimum soil layer impedance
z_T	Kg ·m^{-2} ·s^{-1}	transversal mechanical impedance

7. Bibliography

[1] U.S. Department of Transportation, Federal Transit Administration, *Transit Noise and Vibration Impact Assessment*, Report DOT-T-95-16, April 1995.

[2] A.Crone, T.Astrup, P.Finne, *Prediction of Vibrations and Structure-Borne Noise from Railways*, InterNoise 99, Florida, USA, 1999.

[3] T.Ekevid, M.X.D.Li, N.Wiberg, *Adaptive Finite Element Analysis of Wave Propagation Under Moving Loads Induced by High Speed Trains*, ECCOMAS 2000, Barcelona, September 2000.

[4] H.Takemiya, *Simulation for Vibration Prediction and Mitigation of Track-Ground due to Highspeed Trains - Case of X-2000 in Sweden* -, Informal Workshop at Royal Institute of Technology, Sweden, July 23, 2001.

[5] F.E.Richert, J.R.Hall, *Vibrations of Soils and Foundations*, Prentice-Hall Inc., Englewood Cliffs, NJ, 1970.

[6] C.G.Lai, A.Callerio, E.Faccioli, A.Martino, *Mathematical Modeling of Railway-Induced Ground Vibrations*, WAVE 2000, Bochum, Germany, December 2000.

[7] M.E.Heelis, A.C.Collop, A.R.Dawson, D.N.Chapman, V.Krylov, *Predicting and Measuring Vertical Track Displacements on Soft Subgrades*, Railway Engineering 99, London, May 1999.

[8] L.Fryba, *Vibration of Solids and Structures under Moving Loads*, Telford, London, 1999.
[9] J.P.Fortin, *Dynamic Track Deformation*, French Railway Review, Vol. 1, 1983.
[10] H.Takemiya, *Prediction of Ground Vibration Induced by High-Speed Train Operation*, 18th Sino-Japan Technology Seminar, Taipei, Taiwan, 1997.
[11] D.Le Houdec, *Modelling and Analysis of Ground Vibration Problems: a Review*, Civil and Structural Engineering Computing, Chapter 19, 2001.
[12] H.E.M.Hunt, *Measurement and Modelling of Traffic Induced Ground Vibration*, Ph.D. Thesis, Cambridge University, England, 1988.
[13] T.G.Gutowski, L.E.Wittig, C.L.Dym, *Some Aspects of the Ground Vibration Problem*, Noise Control Engineering, vol. 10:3, 1978.
[14] C.M.Harris, *Shock and Vibration Handbook*, Mc-Graw Hill Professional Publishing, December 1995.
[15] L.L.Beranek, *Noise and Vibration Control*, edited by L.L. Beranek, 1988
[16] G.Mavko, T.Mukerji, J.Dvorkin, *The Rock Physics Handbook*, Cambridge Univ. Press, 1998.
[17] U.S. Army Engineer Waterways Experiment Station, *A Rapid Geophysical Technique for Subbottom Imaging*, Dredging Research, Technical Notes, July 1993.
[18] K.Terzaghi et Al., *Soil Mechanics in Engineering Practice*, John Wiley & Sons, January 1996.
[19] E.Meyer, E.G.Neumann, *Physical and Applied Acoustics*, Academic, London-New York, 1972.
[20] Geo Space, *Geo Space Geophones GS-30CT & GS-32CT*, www.geospacelp.com/gs30ct.htm
[21] DASYTec, *DASYLab User Guide*, www.dasytec.com
[22] A.V.Damiani, G.Minelli, G.Pialli, *L'Unita' Falterona - Trasimeno nell'area compresa fra la Val di Chiana e la Valle Tiberina: Sezione Terontola - Abbazia di Cassiano*, Geological Chart, Studi Geologici Camerti, 2000.
[23] M.E.Heelis, A.C.Collop, A.R.Dawson, D.N.Chapman, V.Krylov, *Resilient Modulus of Soft Soil Beneath High Speed Rail Lines*, Transportation Research Board 99, Washington D.C., January 1999.
[24] U.S. Department of Transportation, Federal Railroad Administration, *High Speed Ground Transportation – Noise and Vibration Impact Assessment*, Report N. 293630-1, December 1998.
[25] M.P.Strohl, *Europe's High Speed Trains*, 1993
[26] H.J.Saurenman, J.T.Nelson, G.P. Wilson, *Handbook of Urban Rail Noise and Vibration Control*, prepared under contract to US DOT/Transportation System Center, Report UMTA-MA-06-0099-82-2, February 1982.